Phospholipase Lpl1 links lipid droplet function with quality control protein degradation

Nina Weisshaar†, Hendrik Welsch†, Angel Guerra-Moreno, and John Hanna*
Department of Pathology, Brigham and Women's Hospital and Harvard Medical School, Boston, MA 02115

ABSTRACT **Protein misfolding is toxic to cells and is believed to underlie many human diseases, including many neurodegenerative diseases. Accordingly, cells have developed stress responses to deal with misfolded proteins. The transcription factor Rpn4 mediates one such response and is best known for regulating the abundance of the proteasome, the complex multisubunit protease that destroys proteins. Here we identify Lpl1 as an unexpected target of the Rpn4 response. Lpl1 is a phospholipase and a component of the lipid droplet. Lpl1 has dual functions: it is required for both efficient proteasome-mediated protein degradation and the dynamic regulation of lipid droplets. Lpl1 shows a synthetic genetic interaction with Hac1, the master regulator of a second proteotoxic stress response, the unfolded protein response (UPR). The UPR has long been known to regulate phospholipid metabolism, and Lpl1's relationship with Hac1 appears to reflect Hac1's role in stimulating phospholipid synthesis under stress. Thus two distinct proteotoxic stress responses control phospholipid metabolism. Furthermore, these results provide a direct link between the lipid droplet and proteasomal protein degradation and suggest that dynamic regulation of lipid droplets is a key aspect of some proteotoxic stress responses.**

Monitoring Editor
William P. Tansey
Vanderbilt University

Received: Oct 13, 2016
Revised: Jan 5, 2017
Accepted: Jan 9, 2017

INTRODUCTION

Misfolded proteins are toxic to cells and are believed to cause or contribute to many human diseases, including most neurodegenerative diseases (Hipp *et al.*, 2014). Accordingly, cells have developed stress responses to identify and destroy misfolded proteins. Two important such pathways are the unfolded protein response (UPR) and the Rpn4 response (Xie and Varshavsky, 2001; Walter and Ron, 2011). The UPR senses misfolded proteins within the endoplasmic reticulum (ER) and responds in a complex manner to mitigate this threat. Central to this response is the activation of the transcription factor Hac1, which mediates a broad transcriptional program to remodel the cell and allow it to better address the proteotoxic threat (Travers *et al.*, 2000). This includes transcription of ER chaperones to promote protein folding, as well as the machinery involved in ER-associated degradation (ERAD) to destroy those proteins that cannot be refolded. The UPR is also capable of down-regulating protein synthesis and, in higher organisms, initiating apoptosis, the latter pathway likely reserved for the most severe cases of proteotoxic stress (Kaufman, 1999; Walter and Ron, 2011). Of interest, for reasons that are not entirely clear, the UPR also stimulates the synthesis of phospholipids (Carman and Han, 2011)

The transcription factor Rpn4 mediates a second proteotoxic stress response that is believed to monitor the functional capacity of the proteasome—the large multisubunit protease that is responsible for most selective protein degradation in eukaryotes (Xie and Varshavsky, 2001). Rpn4 recognizes a consensus motif in the promoters of all known proteasome subunits (Mannhaupt *et al.*, 1999), allowing Rpn4 to orchestrate new proteasome synthesis in a concerted stoichiometric manner. However, Rpn4 is also a substrate of the proteasome with an extremely short half-life (Xie and Varshavsky, 2001). Under conditions that compromise or overwhelm proteasome function, Rpn4 is stabilized. This results in new proteasome synthesis, increasing degradative capacity and eventually restoring rapid degradation of Rpn4, which normalizes the stress response.

This article was published online ahead of print in MBoC in Press (http://www.molbiolcell.org/cgi/doi/10.1091/mbc.E16-10-0717) on January 18, 2017.

†These authors contributed equally.

The authors report no financial conflicts of interest.

*Address correspondence to: John Hanna (jwhanna@partners.org).

Abbreviations used: CPY, carboxypeptidase Y; ER, endoplasmic reticulum; ERAD, ER-associated degradation; LLB, Laemmli loading buffer; PACE, proteasome-associated control element; RT-PCR, reverse transcription PCR; UPR, unfolded protein response.

© 2017 Weisshaar, Welsch *et al.* This article is distributed by The American Society for Cell Biology under license from the author(s). Two months after publication it is available to the public under an Attribution–Noncommercial–Share Alike 3.0 Unported Creative Commons License (http://creativecommons.org/licenses/by-nc-sa/3.0).

"ASCB®," "The American Society for Cell Biology®," and "Molecular Biology of the Cell®" are registered trademarks of The American Society for Cell Biology.

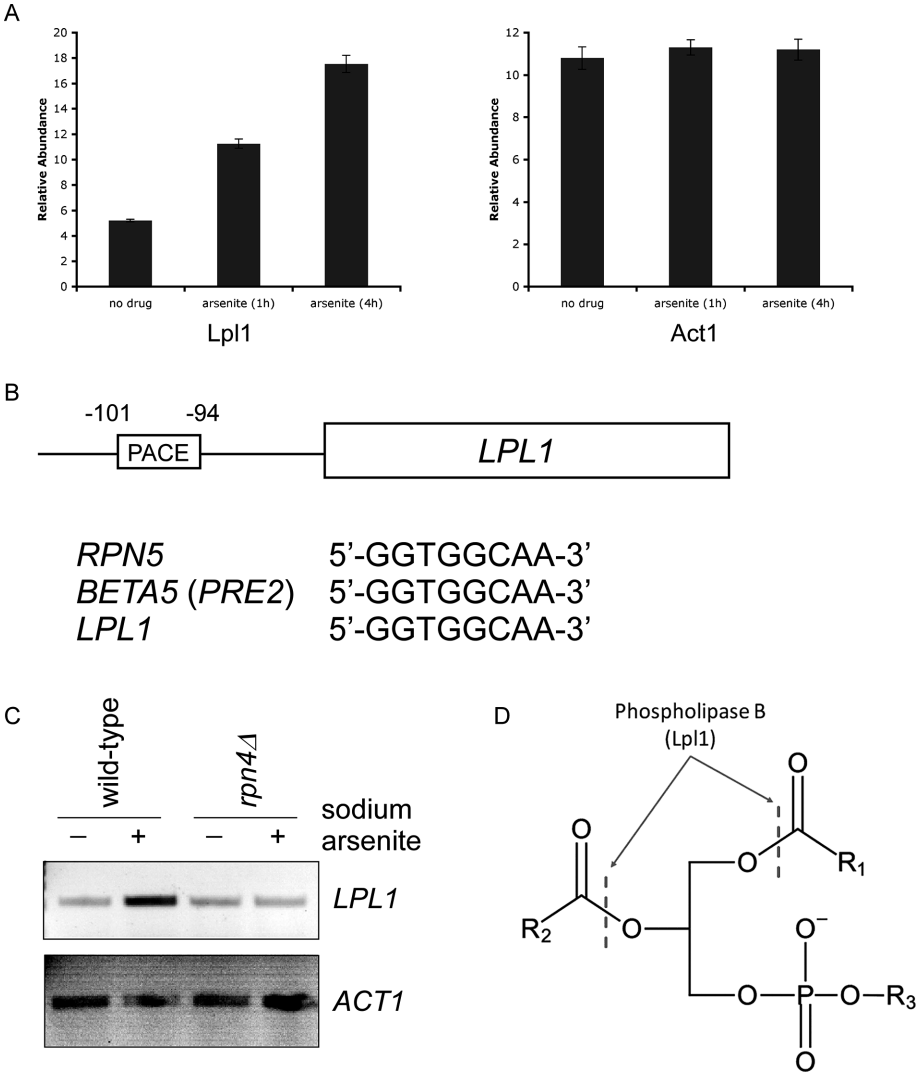

FIGURE 1: Lpl1 is regulated by Rpn4. (A) Relative protein abundance of Lpl1 at 0, 1, and 4 h after treatment with sodium arsenite (1 mM). Data were generated using a tandem mass tag-based mass spectrometry approach (Guerra-Moreno *et al.*, 2015). Act1, a control protein, showed no change. Error bars represent SDs from triplicate cultures. In addition, differences between untreated and treated samples were statistically significant by Student's *t* test ($p < 0.01$) for Lpl1 but not Act1. (B) Schematic diagram of the *LPL1* gene with its associated 5′-untranslated region. A classical PACE motif is present, with its location indicated relative to the start codon. This PACE motif is identical to that of other well-established Rpn4 targets, such as Rpn5 and Beta5 (Pre2). (C) Stress-inducible transcription of *LPL1* in wild-type and *rpn4*Δ cells, as determined by RT-PCR. Treatment was with sodium arsenite (1 mM) for 1 h. *ACT1* (bottom) serves as a control. (D) Schematic of a generic phospholipid with the cleavage sites indicated for type B phospholipases such as Lpl1. R_1 and R_2, fatty acyl groups; R_3, polar head group (e.g., choline, ethanolamine, serine, inositol).

This pathway appears to be functionally conserved in higher organisms, where it is mediated by the transcription factor Nrf1 (Radhakrishnan *et al.*, 2010; Steffen *et al.*, 2010).

The lipid droplet is an organelle-like structure that houses large quantities of neutral lipids (mainly triacylglycerols and sterol esters) and is bounded by a phospholipid monolayer (Radulovic *et al.*, 2013; Wang, 2015). One function of the lipid droplet is believed to be in metabolism—storing and releasing these neutral lipids as needed to meet the cell's energy requirements (Radulovic *et al.*, 2013). However, the lipid droplet remains poorly understood. It has become apparent that the lipid droplet has its own dedicated and complex proteome (Binns *et al.*, 2006). In addition, lipid droplets appear to be dynamic, capable of changing in size and number under different cellular conditions (Fei *et al.*, 2008, 2011). Here we identify the lipid droplet phospholipase Lpl1 as a component of the Rpn4 proteotoxic stress response. Loss of Lpl1 results in multiple proteolytic defects, including synthetic genetic interactions with members of the unfolded protein response. These defects are accompanied by alterations in lipid droplet homeostasis. These results suggest an important role for the lipid droplet in proteotoxic stress responses and provide a direct mechanistic link between these seemingly unrelated pathways.

RESULTS

Lpl1 is a target of the Rpn4 proteotoxic stress response

We recently carried out a proteomic analysis of the cellular response to trivalent arsenic in the yeast *Saccharomyces cerevisiae* (Guerra-Moreno *et al.*, 2015). Under these conditions, Rpn4 protein levels are increased by ~20-fold, and this results in a corresponding increase in the abundance of proteasome subunits. Among the nearly 4600 proteins for which data were available, we noticed that the protein Lpl1 was strongly induced by arsenic in a manner that was similar to some Rpn4 targets (Figure 1A). Rpn4 recognizes its targets through a consensus motif in their promoters known as the proteasome-associated control element (PACE; Mannhaupt *et al.*, 1999). We identified a canonical PACE motif within the *LPL1* promoter that was identical to that of established Rpn4 targets such as Rpn5 and Beta5 (Pre2; Figure 1B). Furthermore, Lpl1's PACE motif was situated within the first 200 nucleotides preceding the start codon, which is the typical location (Leggett *et al.*, 2002). To test directly whether *LPL1* was a transcriptional target of Rpn4, we performed reverse-transcription PCR (RT-PCR) under the same conditions as in Figure 1A. *LPL1* was strongly induced at the RNA level, and this induction was largely dependent on Rpn4 (Figure 1C). Thus Lpl1 is a target of the Rpn4 proteotoxic stress response.

Whereas most known targets of Rpn4 are proteasome subunits or proteasome-interacting proteins, Lpl1 is a component of the lipid droplet (Selvaraju *et al.*, 2014). By sequence and functional analysis, it is a type B phospholipase, allowing it to cleave phospholipids at the sn-1 and sn-2 positions, releasing free fatty acids from the three-carbon backbone, which retains its polar head group (Figure 1D; Selvaraju *et al.*, 2014). Lpl1 showed a relatively broad substrate specificity in vitro, acting on major species such as phosphatidylethanolamine, phosphatidylcholine, and phosphatidylserine, although it showed much lower activity against phosphatidylinositol (Selvaraju *et al.*, 2014).

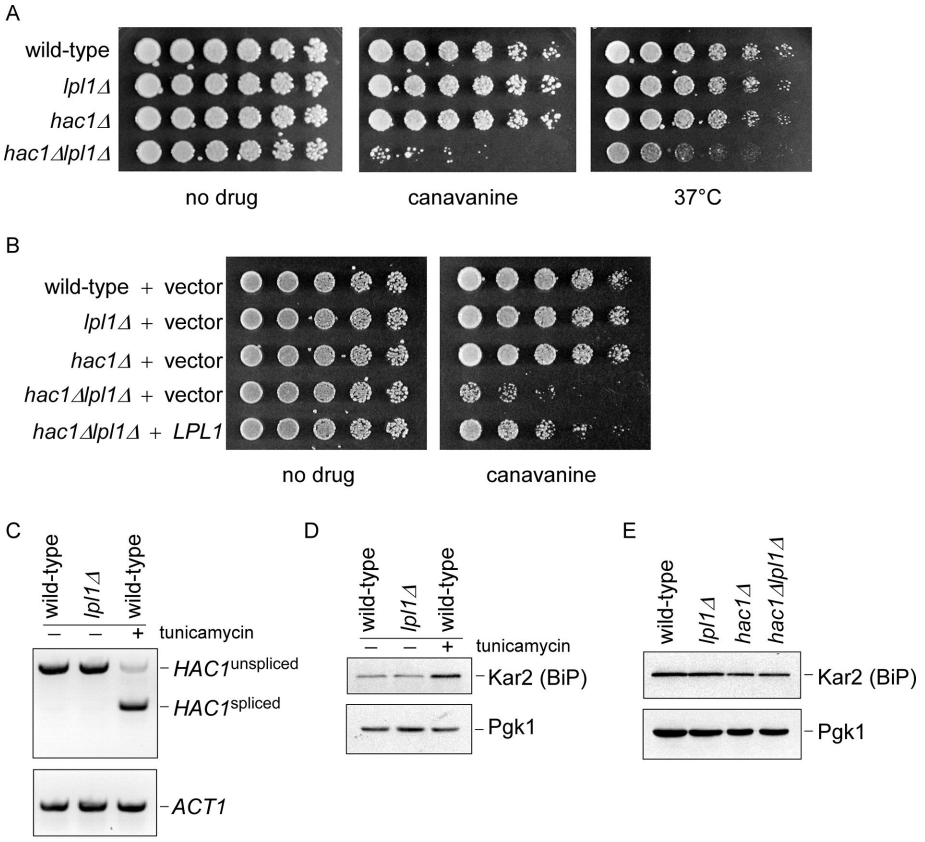

FIGURE 2: Proteotoxic phenotypes of the *hac1*Δ*lpl1*Δ mutant. (A) Growth of wild-type, *lpl1*Δ, *hac1*Δ, and *hac1*Δ*lpl1*Δ strains in the presence of canavanine (1.5 µg/ml) or at elevated temperature, as indicated. Cells were spotted in threefold serial dilutions and cultured for 2–4 d. (B) Growth of wild-type, *lpl1*Δ, *hac1*Δ, and *hac1*Δ*lpl1*Δ strains expressing an empty vector and *hac1*Δ*lpl1*Δ expressing *LPL1* in the presence or absence of canavanine (1.5 µg/ml), as indicated. Cells were spotted in threefold serial dilutions and cultured for 2–4 d at 30°C. (C) Splicing of *HAC1*, as determined by RT-PCR, in wild-type and *lpl1*Δ strains. A wild-type strain treated with tunicamycin (5 µg/ml), an inducer of the unfolded protein response, serves as a positive control. *ACT1* (bottom) serves as a control. (D) Kar2 protein levels in whole-cell extracts of wild-type and *lpl1*Δ strains, as determined by SDS–PAGE followed by immunoblot with anti-Kar2 antibody (top) or anti-Pgk1 antibody (bottom; loading control). (E) Kar2 protein levels in wild-type, *lpl1*Δ, *hac1*Δ, and *hac1*Δ*lpl1*Δ strains. Exponential-phase cells cultured in synthetic medium were treated at 37°C for 1 h. Whole-cell extracts were prepared and analyzed by SDS–PAGE followed by immunoblot with anti-Kar2 antibody (top) or anti-Pgk1 antibody (bottom; loading control).

Functional relationship between Lpl1 and the unfolded protein response

Control of Lpl1 by Rpn4 suggested a potential role for Lpl1 in protein degradation. We examined the *lpl1*Δ mutant for growth defects after exposure to various proteotoxic stresses but were unable to identify a phenotype (unpublished data). However, when *LPL1* was deleted in a *hac1*Δ background, we observed robust phenotypes in response to multiple causes of proteotoxic stress, including elevated temperature and the abnormal amino acid canavanine, which is incorporated into nascent proteins, causing them to misfold (Figure 2A). Hac1 is a transcription factor and a master regulator of the UPR, which is distinct from the Rpn4 response. The UPR responds specifically to misfolded proteins within the ER, and Hac1 orchestrates a complex transcriptional response to mitigate this threat (Travers *et al.*, 2000; Wu *et al.*, 2014). The *hac1*Δ*lpl1*Δ phenotype could be complemented by restoration of plasmid-derived *LPL1*, confirming that the phenotype was indeed caused by loss of Lpl1 (Figure 2B). One potential explanation for such a synthetic phenotype is that the UPR is constitutively induced in the *lpl1*Δ mutant, compensating for defects in this mutant. Hac1 is activated by splicing of its mRNA (Wu *et al.*, 2014). We saw no evidence of increased *HAC1* splicing in the *lpl1*Δ mutant by RT-PCR (Figure 2C). Similarly, the classical UPR target Kar2 (the yeast orthologue of BiP) was not up-regulated at the protein level in the *lpl1*Δ mutant (Figure 2D), although its levels were slightly decreased in the absence of Hac1, as expected (Figure 2E).

Lpl1 functions in protein degradation

The preceding regulatory and phenotypic data suggest a role for Lpl1 in proteasome-mediated protein degradation. Because proteasomes preferentially destroy ubiquitinated proteins, defects in the pathway may lead to an accumulation of high–molecular weight ubiquitin immunoreactive material. Indeed, we observed an accumulation of these ubiquitinated species in the *hac1*Δ*lpl1*Δ mutant, consistent with a significant protein degradation defect (Figure 3A). We next examined a specific protein, CPY*, which is a classical substrate of the ERAD pathway. Wild-type and *lpl1*Δ cells showed similarly rapid degradation of this substrate, with a half-life of <20 min (Figure 3B). CPY* degradation was attenuated in the *hac1*Δ mutant, as expected. Turnover of CPY*, however, was much more strongly attenuated in the *hac1*Δ*lpl1*Δ mutant, which was reflected not only in the rate of turnover, but also in the elevation of steady-state CPY* levels (Figure 3B). This elevation of steady-state protein levels reflects the fact that in a cycloheximide chase assay, where there is no pulse period, the zero time point represents steady-state protein abundance. Thus steady-state levels may increase if there is a strong enough degradative defect or even decrease if there is a strong degradative advantage (Hanna *et al.*, 2006; Guerra-Moreno and Hanna, 2016; Shi *et al.*, 2016). To determine whether this effect was specific to ERAD substrates, we looked at a model cytoplasmic substrate of the proteasome, Δ2-GFP (Kruegel *et al.*, 2011), under similar conditions. This substrate also showed a high rate of degradation, but we did not detect any stabilization in the *lpl1*Δ, *hac1*Δ, or *hac1*Δ*lpl1*Δ mutant (Figure 3C).

Multiple classes of ERAD substrates have been identified, including ER lumenal substrates (such as CPY*) and ER membrane substrates. The 12-transmembrane-domain protein Ste6 is a classical and robust ERAD substrate. In wild-type cells, expression of mutant Ste6 does not produce a growth defect, as these cells can rapidly destroy misfolded Ste6 (Metzger and Michaelis, 2009). However, mutants defective in Ste6 degradation show growth defects that reflect the underlying toxicity of this misfolded protein. We expressed mutant *ste6-Q1249X* in these strains, along with wild-type Ste6 as a control. Wild-type and *lpl1*Δ cells showed no defect (Figure 3D). By contrast, the *hac1*Δ mutant showed a growth defect, consistent with a defect in Ste6 degradation. Again, this defect was

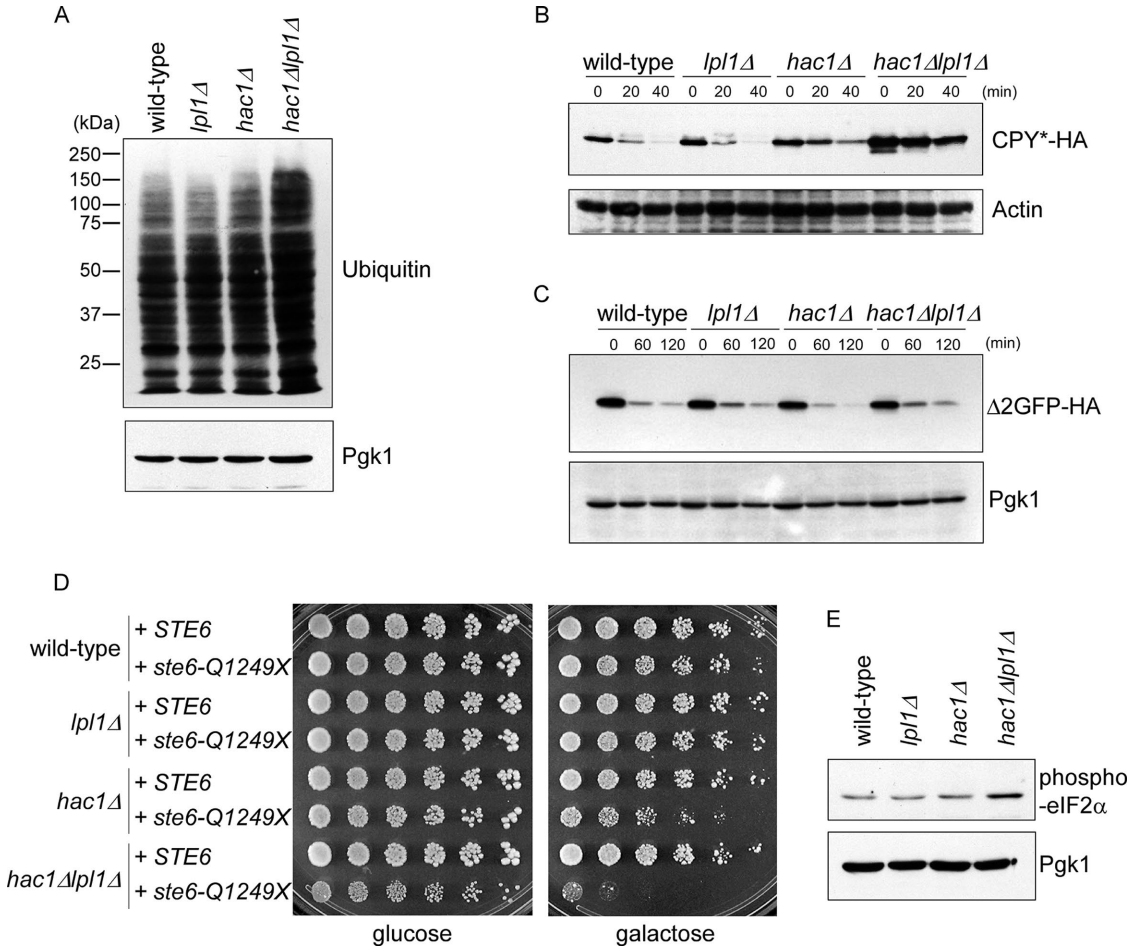

FIGURE 3: Protein degradation defects in the *hac1Δlpl1Δ* mutant. (A) Levels of ubiquitin conjugates in whole-cell extracts of wild-type, *lpl1Δ*, *hac1Δ*, and *hac1Δlpl1Δ* strains, as determined by SDS–PAGE followed by immunoblot with anti-ubiquitin antibody (top) or anti-Pgk1 antibody (bottom; loading control). Experiment was performed at 37°C. (B) Cycloheximide chase analysis of CPY* turnover in wild-type, *lpl1Δ*, *hac1Δ*, and *hac1Δlpl1Δ* strains, as determined by SDS–PAGE followed by immunoblot with anti-HA antibody (top) or anti-actin antibody (bottom; loading control). Experiment was performed at 37°C. See Supplemental Figure S1 for quantitation. (C) Cycloheximide chase analysis of turnover of the cytoplasmic proteasome substrate Δ2-GFP, as determined by SDS–PAGE followed by immunoblot with anti-HA antibody (top) or anti-Pgk1 antibody (bottom; loading control). Experiment was performed at 37°C. (D) Growth of wild-type, *lpl1Δ*, *hac1Δ*, and *hac1Δlpl1Δ* strains expressing galactose-inducible wild-type *STE6* or the misfolded mutant *ste6-Q1249X*. Cells were spotted in threefold serial dilutions and cultured for 4 d at 35°C. (E) Levels of phosphorylated eIF2α (Ser-51) in whole-cell extracts of wild-type, *lpl1Δ*, *hac1Δ*, and *hac1Δlpl1Δ* strains treated with sodium arsenite (0.2 mM), as determined by SDS–PAGE followed by immunoblot with anti–phospho-eIF2α antibody (top) or anti-Pgk1 antibody (bottom; loading control). Experiment was performed at 37°C.

dramatically exacerbated in the *hac1Δlpl1Δ* double mutant (Figure 3D). One useful aspect of this assay is that it integrates specific degradation defects with an in vivo readout of physiological relevance.

A hallmark of many proteotoxic stressors is the phosphorylation of the translation initiation factor eIF2α at serine-51, a pathway referred to as the integrated stress response (Kaufman, 1999). This phosphorylation inhibits eIF2 function, thereby limiting protein synthesis by the ribosome. Under conditions in which protein misfolding is prevalent, reducing the synthesis of new proteins may be advantageous. The UPR, for example, has long been known to promote eIF2α phosphorylation (Kaufman, 1999). We recently showed that trivalent arsenic is a potent inducer of eIF2α phosphorylation in yeast (Guerra-Moreno *et al.*, 2015), although the underlying mechanism is unknown. We monitored eIF2α phosphorylation in these strains after arsenic treatment. The *hac1Δlpl1Δ* mutant showed increased levels of eIF2α phosphorylation (Figure 3E), compatible with an underlying defect in proteotoxic stress response in this mutant. Taken together, these data suggest an important role for Lpl1 in quality control protein degradation by the proteasome.

Relationship between Lpl1 and phospholipid metabolism

To obtain a better understanding of the role of Lpl1 in protein degradation, we sought to understand the basis for the relationship between Lpl1 and Hac1. According to microarray and other analyses, the UPR and Hac1 have potentially hundreds of transcriptional targets (Travers *et al.*, 2000). These targets fall into a smaller number of categories, including ER chaperones, dedicated ERAD components, secretory pathway genes, phospholipid metabolism genes, and others (Figure 4A). Control of phospholipid synthesis by the UPR has been recognized for almost 20 years (Cox *et al.*, 1997; Kaufman, 1999), although its precise role in counteracting proteotoxic stress has remained somewhat unclear. Naturally, this aspect of the UPR

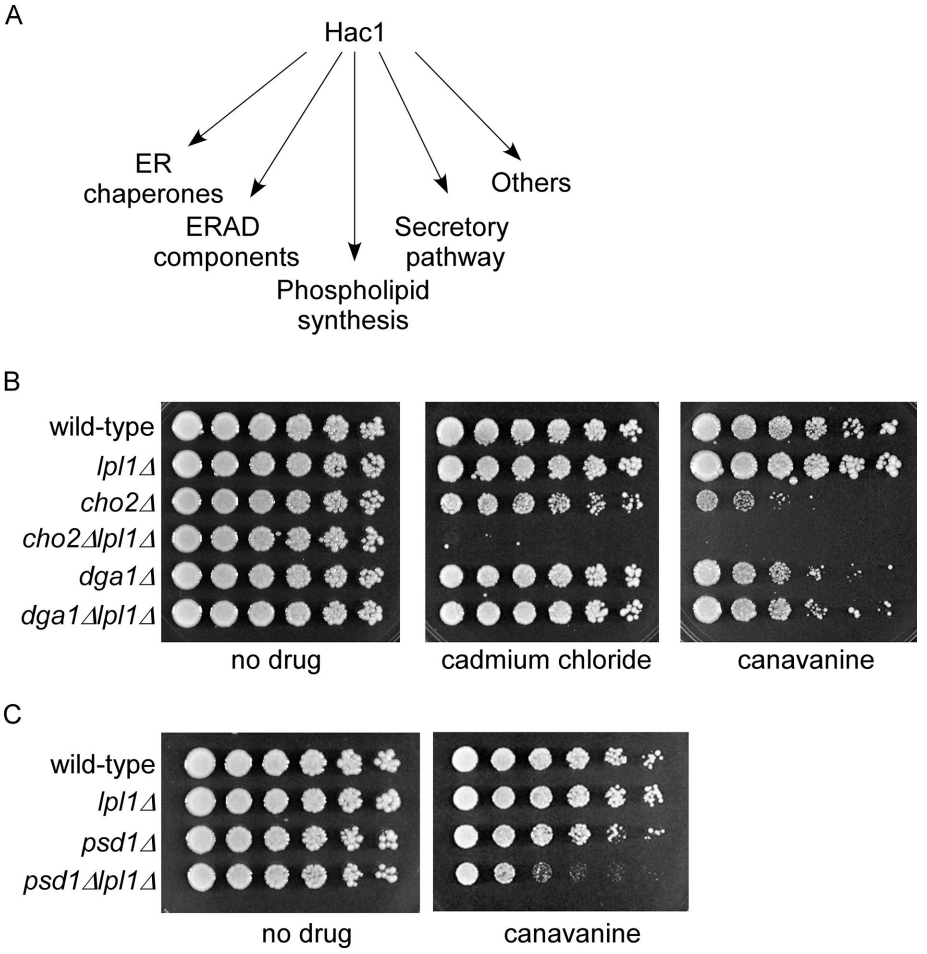

FIGURE 4: Proteotoxic phenotypes of *cho2*Δ*lpl1*Δ and *psd1*Δ*lpl1*Δ mutants. (A) Major classes of transcriptional targets for Hac1. (B) Growth of wild-type, *lpl1*Δ, *cho2*Δ, *cho2*Δ*lpl1*Δ, *dga1*Δ, and *dga1*Δ*lpl1*Δ strains in the presence of cadmium chloride (30 μM) or canavanine (1.5 μg/ml), as indicated. Cells were spotted in threefold serial dilutions and cultured at 30°C for 2–9 d. (C) Growth of wild-type, *lpl1*Δ, *psd1*Δ, and *psd1*Δ*lpl1*Δ strains in the presence or absence of canavanine (1.5 μg/ml), as indicated. Cells were spotted in threefold serial dilutions and cultured at 30°C for 2–4 d.

was intriguing, given that Lpl1 also functions in phospholipid metabolism. The Hac1 target Cho2 promotes synthesis of phosphatidylcholine, an abundant membrane phospholipid, from phosphatidylethanolamine. We constructed a *cho2*Δ*lpl1*Δ double mutant and tested its ability to survive various proteotoxic stressors. The *cho2*Δ*lpl1*Δ mutant showed strong sensitivities to canavanine, phenocopying the *hac1*Δ*lpl1*Δ mutant (Figure 4B). We also detected a strong growth defect of *cho2*Δ*lpl1*Δ on cadmium chloride, a divalent heavy metal and another well-established cause of proteotoxicity (Seufert and Jentsch, 1990). To gauge the specificity of this interaction, we looked at Dga1, which is also involved in lipid metabolism but functions in the unrelated triacylglycerol synthesis pathway and is not a known target of the UPR. In contrast, a *dga1*Δ*lpl1*Δ mutant showed no effect under these conditions (Figure 4B). It is worth noting that the *cho2*Δ mutant alone showed sensitivity under these conditions, suggesting some degree of proteotoxic stress defect on its own (Figure 4B; see also Thibault *et al.*, 2012).

Psd1 functions upstream of Cho2, promoting conversion of phosphatidylserine to phosphatidylethanolamine. We tested a *psd1*Δ*lpl1*Δ mutant, which also showed a growth defect when treated with canavanine (Figure 4C), although the severity of the phenotype was less than that of *cho2*Δ*lpl1*Δ. We did not detect synthetic genetic effects when *lpl1*Δ was combined with other mutants of the UPR such as Hrd1, a core component of the ERAD pathway, or Ino1, which mediates phosphatidylinositol synthesis via a metabolic pathway distinct from that which synthesizes phosphatidylserine, phosphatidylethanolamine, and phosphatidylcholine (unpublished data).

Modulation of lipid droplet dynamics by Lpl1

Lipid droplets are small, organelle-like structures in which a phospholipid monolayer surrounds a core of mostly neutral lipids, principally triacylglycerols and sterol esters. They can be visualized using fluorescence microscopy (Thibault *et al.*, 2012; Selvaraju *et al.*, 2014). In wild-type cells under normal conditions, there are typically 5–10 distinct lipid droplets per cell, and these are small and uniform in size. *cho2*Δ cells show extremely large lipid droplets, which can be up to 50 times the volume of wild-type lipid droplets (Fei *et al.*, 2011). These cells also have many fewer lipid droplets and, in many cases, only a single dominant lipid droplet.

We confirmed the finding of supersized lipid droplets in *cho2*Δ cells (Figure 5A), which frequently showed a single massive lipid droplet, with few or no accompanying smaller lipid droplets. This type of lipid droplet was virtually never seen in wild-type cells. The *lpl1*Δ mutant appeared similar to wild type. However, loss of Lpl1 in the *cho2*Δ background markedly altered the lipid droplet profile (Figure 5, A and B). The number of cells with a single dominant lipid droplet was reduced. In their place were cells with lipid droplets that were greater in number but smaller in size than the supersized lipid droplets of *cho2*Δ (Figure 5, A and B). Because these lipid droplets were still larger than those seen in wild-type cells, we referred to this pattern as "intermediate." It is worth noting that such intermediate-type cells can be seen in the *cho2*Δ mutant (see also Fei *et al.*, 2011), but their abundance is significantly increased upon loss of Lpl1. These findings indicate that Lpl1 functions in the dynamic regulation of lipid droplets. Furthermore, the partial restoration of the *cho2*Δ phenotype suggests that Lpl1 may be required for the formation of supersized lipid droplets in the *cho2*Δ mutant.

Relationship between Rpn4 and phospholipid metabolism

Stress-inducible expression of Lpl1 is dependent on Rpn4 (Figure 1, B and C). Thus the preceding data on Lpl1 suggest a potential relationship between phospholipid metabolism and the Rpn4 proteotoxic stress response, a possibility that has not been previously considered. We therefore examined the consequences of compromising phospholipid metabolism in the *rpn4*Δ mutant. First, we found that the *rpn4*Δ *cho2*Δ mutant showed a strong growth defect when protein misfolding was broadly induced by canavanine (Figure 6A).

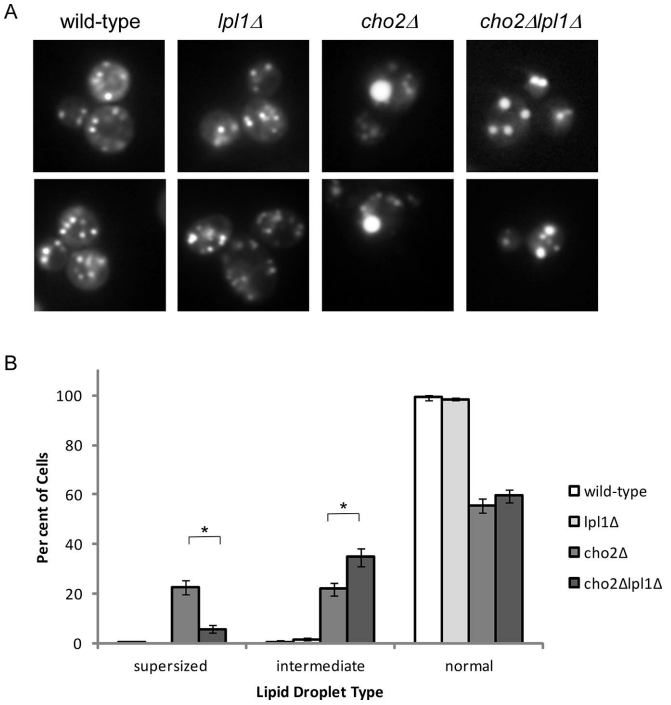

FIGURE 5: Lpl1 affects lipid droplet dynamics. (A) Representative images of lipid droplets, as visualized by fluorescence microscopy for the indicated strains. *cho2*Δ cells show a relative accumulation of cells with a single very large ("supersized") lipid droplet. *cho2*Δ*lpl1*Δ cells show a relative accumulation of cells with an intermediate phenotype (i.e., lipid droplets that are smaller but more numerous than those seen in *cho2*Δ). (B) Quantitation of normal, intermediate, and supersized lipid droplets. Six hundred cells were counted (in 100 cell groups) for each strain. Error bars represent SDs. Asterisk, statistically significant by Student's *t* test ($p < 0.001$).

Next we used the Ste6 assay to determine the effect of a single defined misfolded protein on this mutant. Here we used two distinct Ste6 mutants: L1239X and Q1249X. *rpn4*Δ alone showed sensitivity to both misfolded proteins, as previously reported (Metzger and Michaelis, 2009). However, when combined with the *cho2*Δ mutant, growth was markedly diminished (Figure 6B). Finally, we examined whether loss of Rpn4 could recapitulate Lpl1's effects on lipid droplets. Indeed, loss of Rpn4 partially reversed the lipid-droplet phenotype of the *cho2*Δ mutant, again resulting in an increase in the percentage of cells with an intermediate phenotype (Figure 6, C and D). These findings suggest that two separate proteotoxic stress responses—the Rpn4 response and the UPR—are closely linked to phospholipid metabolism and lipid droplet function.

DISCUSSION

Novel aspects of the Rpn4 proteotoxic stress response

Rpn4's best-known function is the coordinated regulation of proteasome biosynthesis (Mannhaupt *et al.*, 1999; Xie and Varshavsky, 2001). Accordingly, Rpn4's major known transcriptional targets include the ~35 subunits of the proteasome, as well as an increasing number of proteasome-associated proteins that may be present in substoichiometric amounts or associate reversibly (Mannhaupt *et al.*, 1999; Leggett *et al.*, 2002; Sa-Moura *et al.*, 2013; Hanna *et al.*, 2014). Thus Lpl1 is a quite unusual transcriptional target for Rpn4. Our assignment of Lpl1 as an Rpn4 effector is supported by two prior microarray studies that detected transcriptional induction of *LPL1* in response to different proteotoxic stressors, although no further analysis of Lpl1 was reported (Fleming *et al.*, 2002; Metzger and Michaelis, 2009).

Our results suggest a broader role for Rpn4 in proteotoxic stress responses than was previously anticipated. Indeed, bioinfomatics analyses have identified potential PACE motifs in the promoters of many nonproteasomal genes (Mannhaupt *et al.*, 1999; Shirozu *et al.*, 2015). Moreover, transcriptional profiling experiments indicate many more potential Rpn4 targets, possibly numbering in the hundreds (Jelinsky *et al.*, 2000). The determination of the full breadth and function of the Rpn4 response remains an important goal for future work and will ultimately require a comprehensive analysis of the function of each Rpn4 effector.

Role of phospholipid metabolism in proteotoxic stress responses

The Rpn4 response and the UPR appear to represent largely distinct pathways. Proteasome subunits, for example, are not direct transcriptional targets of the UPR (Travers *et al.*, 2000). Similarly, the dedicated ERAD components controlled by the UPR (e.g., Hrd1, Hrd3, and Ubc7) are not targets of Rpn4. Our work suggests a novel and interesting parallel between the two pathways: each regulates phospholipid metabolism. The UPR stimulates phospholipid synthesis, whereas Rpn4 regulates phospholipid breakdown via Lpl1. The precise role of phospholipid synthesis in the UPR has remained somewhat unclear. An attractive model is that protein misfolding in the ER may be mitigated by expanding the compartment, in effect diluting the concentration of misfolded proteins (Schuck *et al.*, 2009). Because phospholipids are major constituents of membranes, new phospholipid synthesis may be required for this process. An alternate model, not mutually exclusive, is that remodeling of membranes could alter the folding environment within the ER, providing a better environment for protein folding. This could proceed by altering the physicochemical properties of membranes, for example, by changing the hydrophobicity, length, or degree of unsaturation of membrane phospholipids.

An interesting aspect of Lpl1 is that its role in protein degradation became apparent only after compromising the UPR in the *hac1*Δ mutant. Hac1 regulates many different cellular processes and controls the expression of potentially hundreds of genes (Kaufman, 1999; Travers *et al.*, 2000). In principle, dysregulation of any of these genes could represent the basis for the *hac1*Δ*lpl1*Δ mutant. Our data suggest that Hac1's control of phospholipid synthesis is particularly relevant for Lpl1 function. This is supported by the observation that impairing phospholipid synthesis in the *cho2*Δ*lpl1*Δ and the *psd1*Δ*lpl1*Δ mutants phenocopies the *hac1*Δ*lpl1*Δ mutant (Figure 4, B and C). A simple model is that recycling of lipid droplet phospholipids by Lpl1 provides precursor products that can be used in new phospholipid synthesis. In this regard, the lipid droplet, in addition to storing neutral lipids, may also serve as a functional reservoir of phospholipids. Alternatively, and not mutually exclusive, the free fatty acids liberated by Lpl1 (Figure 1D) could be used in another process, such as energy production via beta oxidation or lipid modification of proteins (e.g., myristoylation). Further work is needed to test these models.

Role of Lpl1 in lipid droplet function

The lipid droplet is bounded by a phospholipid monolayer. Lpl1 appears to break down these phospholipids (Selvaraju *et al.*, 2014), and this loss might be expected to result in smaller lipid droplet particles. By contrast, we see that the accumulation of very large lipid droplets in the *cho2*Δ mutant is partially dependent on Lpl1

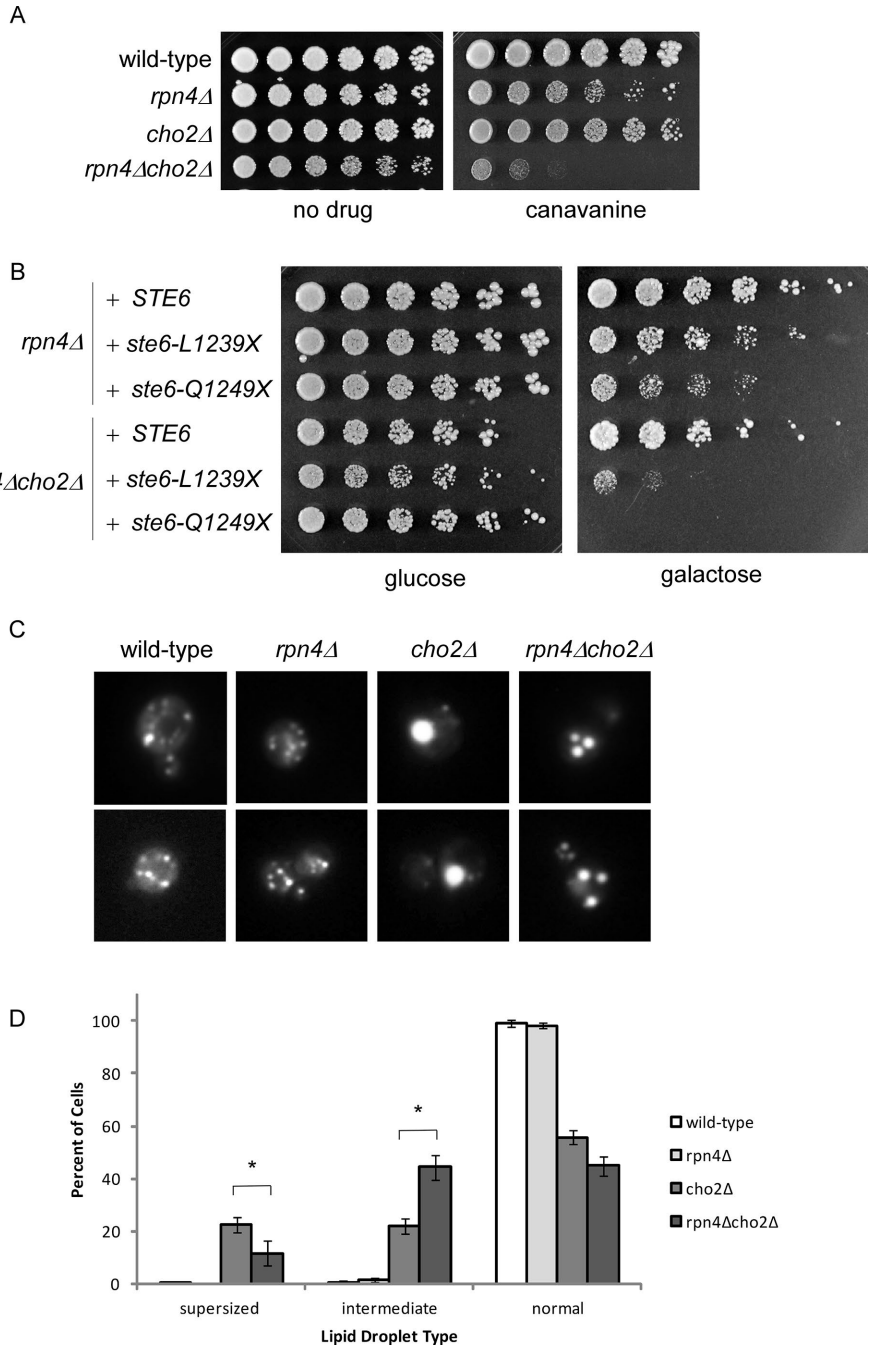

FIGURE 6: Rpn4 recapitulates aspects of Lpl1 function. (A) Growth of wild-type, *rpn4*Δ, *cho2*Δ, and *rpn4*Δ*cho2*Δ strains in the presence of canavanine (0.5 µg/ml). Cells were spotted in threefold serial dilutions and cultured at 30°C for 2–4 d. Note that a lower concentration of canavanine was used here than in Figure 4B. (B) Growth of *rpn4*Δ and *rpn4*Δ*cho2*Δ strains expressing galactose-inducible wild-type *STE6* or the misfolded mutant *ste6-L1239X* or *ste6-Q1249X*. Cells were spotted in threefold serial dilutions and cultured for 4 d at 33°C. The *cho2*Δ mutant alone did not show a phenotype under these conditions (unpublished data). (C) Representative images of lipid droplets, as visualized by fluorescence microscopy, for the indicated strains. *cho2*Δ cells show a relative accumulation of cells with a single very large ("supersized") lipid droplet. Similar to *cho2*Δ*lpl1*Δ, *rpn4*Δ*cho2*Δ cells show a relative accumulation of cells with an intermediate phenotype (i.e., lipid droplets that are smaller but more numerous than those seen in *cho2*Δ). (D) Quantitation of normal, intermediate, and supersized lipid droplets. Six hundred cells were counted (in 100 cell groups) for each strain. Error bars represent SDs. Asterisk, statistically significant by Student's *t* test ($p < 0.001$). Note that all six strains represented in Figures 5A and 6C were analyzed as a group. Thus the values for wild-type and *cho2*Δ are the same in both.

(Figure 5, A and B). Similarly, simply overexpressing Lpl1 in a wild-type background resulted in larger lipid droplet size (Selvaraju *et al.*, 2014). A key observation in this regard is that the increase in lipid droplet size in the *cho2*Δ mutant is accompanied by a decrease in the number of lipid droplet particles per cell (Figure 5A; Fei *et al.*, 2011). Thus a straightforward explanation for the seemingly paradoxical effect of Lpl1 is that lipid droplet catabolism by Lpl1 is accompanied by fusion of the smaller lipid droplet particles, resulting in larger but fewer lipid droplets in the cell. Proteomic analysis indicates that Lpl1 is significantly induced in the *cho2*Δ mutant (see Supplemental Table 3 of Thibault *et al.*, 2012), further supporting this notion. This also suggests that formation of supersized lipid droplets in the *cho2*Δ mutant may be part of a protective response related to phospholipid deficiency. Indeed, supersized lipid droplets are seen only when *cho2*Δ cells are cultured in synthetic (i.e., minimal) media (Fei *et al.*, 2011; unpublished data). They are not seen in rich media, presumably because cells can take up precursor products from the extracellular environment and synthesize phospholipids through the alternate Kennedy pathway (Carman and Han, 2011).

Why lipid droplet fusion should occur is unclear. The lipid droplet houses large quantities of neutral lipids, and the phospholipid monolayer ensures that this densely hydrophobic core is shielded from the aqueous environment. Lipid droplet fusion thus may be a response to ensure the integrity of the particle as phospholipids become limiting within the monolayer. Modeled as a sphere, the ratio of volume to surface area should increase as the diameter of the lipid droplet increases. How lipid droplet fusion could occur and whether this is a regulated process also remain unclear. At least one report suggests that purified lipid droplets in vitro could fuse without supplementing ATP or cytoplasmic constituents (Fei *et al.*, 2008).

Relationships between proteotoxic stress, lipid metabolism, and human disease

The role of protein quality control in human disease is well established, particularly in the family of neurodegenerative diseases that are believed to be caused by the toxic accumulation of misfolded proteins. However, a number of intriguing clinical and basic observations over many years has linked proteotoxic stress responses, particularly the unfolded protein response, to diseases

Strain	Genotype	Reference
BY4741	*MATa his3Δ1 leu2Δ0 met15Δ0 ura3Δ0*	RG Collection
rpn4Δ	*MATa his3Δ1 leu2Δ0 met15Δ0 ura3Δ0 rpn4::KAN*	RG Collection
lpl1Δ	*MATa his3Δ1 leu2Δ0 met15Δ0 ura3Δ0 lpl1::KAN*	RG Collection
hac1Δ	*MATa his3Δ1 leu2Δ0 met15Δ0 ura3Δ0 hac1::KAN*	RG Collection
sJH522	*MATa his3Δ1 leu2Δ0 met15Δ0 ura3Δ0 hac1::KAN lpl1::HYG*	This study
sJH536	*MATa his3Δ1 leu2Δ0 met15Δ0 ura3Δ0* [ycPlac33]	This study
sJH537	*MATa his3Δ1 leu2Δ0 met15Δ0 ura3Δ0 lpl1::KAN* [ycPlac33]	This study
sJH538	*MATa his3Δ1 leu2Δ0 met15Δ0 ura3Δ0 hac1::KAN* [ycPlac33]	This study
sJH539	*MATa his3Δ1 leu2Δ0 met15Δ0 ura3Δ0 hac1::KAN lpl1::HYG* [ycPlac33]	This study
sJH540	*MATa his3Δ1 leu2Δ0 met15Δ0 ura3Δ0 hac1::KAN lpl1::HYG* [pJH197]	This study
sJH559	*MATa his3Δ1 leu2Δ0 met15Δ0 ura3Δ0* [pSM1763]	This study
sJH560	*MATa his3Δ1 leu2Δ0 met15Δ0 ura3Δ0 lpl1::KAN* [pSM1763]	This study
sJH561	*MATa his3Δ1 leu2Δ0 met15Δ0 ura3Δ0 hac1::KAN* [pSM1763]	This study
sJH562	*MATa his3Δ1 leu2Δ0 met15Δ0 ura3Δ0 hac1::KAN lpl1::HYG* [pSM1763]	This study
sJH571	*MATa his3Δ1 leu2Δ0 met15Δ0 ura3Δ0* [pJH146]	This study
sJH572	*MATa his3Δ1 leu2Δ0 met15Δ0 ura3Δ0 lpl1::KAN* [pJH146]	This study
sJH573	*MATa his3Δ1 leu2Δ0 met15Δ0 ura3Δ0 hac1::KAN* [pJH146]	This study
sJH574	*MATa his3Δ1 leu2Δ0 met15Δ0 ura3Δ0 hac1::KAN lpl1::HYG* [pJH146]	This study
sJH630	*MATa his3Δ1 leu2Δ0 met15Δ0 ura3Δ0* [pSM1897]	This study
sJH631	*MATa his3Δ1 leu2Δ0 met15Δ0 ura3Δ0* [pSM2213]	This study
sJH632	*MATa his3Δ1 leu2Δ0 met15Δ0 ura3Δ0 lpl1::KAN* [pSM1897]	This study
sJH633	*MATa his3Δ1 leu2Δ0 met15Δ0 ura3Δ0 lpl1::KAN* [pSM2213]	This study
sJH634	*MATa his3Δ1 leu2Δ0 met15Δ0 ura3Δ0 hac1::KAN* [pSM1897]	This study
sJH635	*MATa his3Δ1 leu2Δ0 met15Δ0 ura3Δ0 hac1::KAN* [pSM2213]	This study
sJH636	*MATa his3Δ1 leu2Δ0 met15Δ0 ura3Δ0 hac1::KAN lpl1::HYG* [pSM1897]	This study
sJH637	*MATa his3Δ1 leu2Δ0 met15Δ0 ura3Δ0 hac1::KAN lpl1::HYG* [pSM2213]	This study
cho2Δ	*MATa his3Δ1 leu2Δ0 met15Δ0 ura3Δ0 cho2::KAN*	RG Collection
sJH575	*MATa his3Δ1 leu2Δ0 met15Δ0 ura3Δ0 cho2::KAN lpl1::HYG*	This study
dga1Δ	*MATa his3Δ1 leu2Δ0 met15Δ0 ura3Δ0 dga1::KAN*	RG Collection
sJH576	*MATa his3Δ1 leu2Δ0 met15Δ0 ura3Δ0 dga1::KAN lpl1::HYG*	This study
psd1Δ	*MATa his3Δ1 leu2Δ0 met15Δ0 ura3Δ0 psd1::KAN*	RG Collection
sJH598	*MATa his3Δ1 leu2Δ0 met15Δ0 ura3Δ0 psd1::KAN lpl1::HYG*	This study
sJH612	*MATa his3Δ1 leu2Δ0 met15Δ0 ura3Δ0 cho2::KAN rpn4::NAT*	This study
sJH614	*MATa his3Δ1 leu2Δ0 met15Δ0 ura3Δ0 rpn4::KAN* [pSM1897]	This study
sJH615	*MATa his3Δ1 leu2Δ0 met15Δ0 ura3Δ0 rpn4::KAN* [pSM2212]	This study
sJH616	*MATa his3Δ1 leu2Δ0 met15Δ0 ura3Δ0 rpn4::KAN* [pSM2213]	This study
sJH638	*MATa his3Δ1 leu2Δ0 met15Δ0 ura3Δ0 cho2::KAN rpn4::NAT* [pSM1897]	This study
sJH639	*MATa his3Δ1 leu2Δ0 met15Δ0 ura3Δ0 cho2::KAN rpn4::NAT* [pSM2212]	This study
sJH640	*MATa his3Δ1 leu2Δ0 met15Δ0 ura3Δ0 cho2::KAN rpn4::NAT* [pSM2213]	This study

Research Genetics (RG) Collection strains are available from ThermoFisher Scientific.

TABLE 1: Yeast strains.

of lipid metabolism, including obesity, insulin resistance, and diabetes (Hummasti and Hotamisligil, 2010; Volmer and Ron, 2015). For example, obesity is associated with induction of the unfolded protein response (Ozcan *et al.*, 2004), and weight loss correlates with reduced ER stress (Gregor *et al.*, 2009). Conversely, mutants deficient in the unfolded protein response develop insulin resistance (Ozcan *et al.*, 2004). These relationships between protein degradation, lipid metabolism, and dyslipidemia remain poorly understood

Plasmid	Details	Reference
ycPlac33	Empty vector (CEN/URA3)	Gietz and Sugino (1988)
pJH197	*LPL1* (in ycPlac33, CEN/URA3)	This study
pSM1763	*CPY*-HA* (CEN/URA3)	Huyer *et al.* (2004)
pJH146	Δ2-GFP-HA (HIS3)	Kruegel *et al.* (2011)
pSM1897	p^{GAL1}STE6-GFP (2μ/*URA3*)	Metzger and Michaelis (2009)
pSM2213	p^{GAL1}*ste6-Q1249X* (2μ/*URA3*)	Metzger and Michaelis (2009)
pSM2212	p^{GAL1}*ste6-L1239X* (2μ/*URA3*)	Metzger and Michaelis (2009)

TABLE 2: Yeast plasmids.

at a molecular level. Lpl1 directly links proteotoxic stress responses to lipid droplet function and thus provides a mechanistic basis for further understanding these complex relationships between protein degradation and lipid metabolism.

MATERIALS AND METHODS

Strains and plasmids

Yeast strains and plasmids are listed in Tables 1 and 2, respectively. Standard techniques were used for strain constructions and transformations. YPD medium consisted of 1% yeast extract, 2% Bacto-peptone, and 2% dextrose. Synthetic medium consisted of 0.7% Difco Yeast Nitrogen Base supplemented with amino acids, adenine, uracil, and 2% dextrose. Where appropriate, the relevant amino acid or nucleic acid was omitted for plasmid selection. Where appropriate, 2% galactose was used instead of dextrose to induce gene expression.

Proteomic analysis

Proteomic analysis to determine the cellular response to trivalent arsenic was previously performed using a tandem mass tag-based mass spectrometry approach and was described in detail (Guerra-Moreno *et al.*, 2015). Data for nearly 4600 proteins were obtained in triplicate at 0, 1, and 4 h after treatment. The data shown here for Lpl1 represent further original analysis of that data set.

RT-PCR

RT-PCR was carried out as previously described (Guerra-Moreno and Hanna, 2016). *LPL1* was amplified with the primers 5-AATGAGGTCAGAGGAAAATTAGG-3 and 5-TCAATTACTCTTGTGCATCAAG-3. *ACT1* was amplified with the primers 5-CTGGTATGTTCTAGCGCTTG-3 and 5-GATACCTTGGTGTCTTGGTC-3. *HAC1* was amplified with the primers 5-CACTCGTCGTCTGATACG-3 and 5-CATTCAATTCAAATGAATTCAAACCTG-3. These primers amplify unspliced and spliced *HAC1* species. As a positive control for *HAC1* splicing, cells were treated with tunicamycin at 5 μg/ml for 1 h.

Phenotypic analysis

Cells from overnight cultures were standardized by optical density and spotted in threefold serial dilutions onto the indicated plates and incubated at the indicated temperatures.

Degradation assays and immunoblot analysis

To analyze total ubiquitin conjugates, whole-cell extracts were prepared from exponential-phase cultures. Cells were normalized by optical density; cell pellets were resuspended in 1× Laemmli loading buffer (LLB) and boiled for 5 min. For all other immunoblots, extracts were prepared by a lithium acetate/sodium hydroxide method as follows. Exponential-phase cultures were normalized by optical density, treated with 2 M lithium acetate on ice for 5 min, and then treated with 0.4 M sodium hydroxide on ice for 5 min. Cell pellets were resuspended in 1× LLB and boiled for 5 min. Analysis was by standard SDS–PAGE followed by immunoblotting. For cycloheximide chase analyses, cycloheximide (100 μg/ml) was added at time 0 to inhibit protein synthesis, and extracts were prepared as described at the indicated time points. Note that the experiments of Figure 3, A–C and E, were carried out at 37°C. Where indicated, the unfolded protein response was induced by treating cells with tunicamycin at 5 μg/ml for 1 h.

The following antibodies were used: anti-ubiquitin (SC-8017; Santa Cruz Biotechnology), anti-Pgk1 (459250; Invitrogen), anti–HA-peroxidase (12013819001; Roche), anti-actin (MA511866; ThermoFisher), anti–phospho-eIF2α (9721S; Cell Signaling Technology), and anti-Kar2 (sc-33630; Santa Cruz Biotechnology).

Lipid droplet fluorescence microscopy

Logarithmically growing cells were cultured in minimal medium and shifted to 37°C for 1 h before harvesting. Cells were fixed with 2% formaldehyde and incubated with 0.5 μg/ml BODIPY 493/503 (ThermoFisher Scientific; Selvaraju *et al.*, 2014). Lipid droplets were visualized by fluorescence microscopy using an Olympus BX51 microscope outfitted with a 100× oil immersion objective and the appropriate filters.

To quantify lipid droplets, six groups of 100 cells each were counted sequentially over multiple days for each strain. The normal pattern consisted of 5–10 small dispersed lipid droplets per cell. The "supersized" pattern consisted of a single dominant lipid droplet, typically with no other visible lipid droplets or 1 or 2 small lipid droplets. The intermediate pattern consisted of 2–5 lipid droplets that were intermediate in size between normal and supersized. Lipid droplet distributions were analyzed by SD and two-tailed Student's *t* test.

ACKNOWLEDGMENTS

We thank Susan Michaelis and Marion Schmidt for plasmids and Daniel Finley and members of the Hanna lab for comments on the manuscript. This work was supported by National Institutes of Health Grant DP5-OD019800.

REFERENCES

Binns D, Januszewski T, Chen Y, Hill J, Markin VS, Zhao Y, Gilpin C, Chapman KD, Anderson RG, Goodman JM (2006). An intimate collaboration between peroxisomes and lipid bodies. J Cell Biol 173, 719–731.

Carman GM, Han GS (2011). Regulation of phospholipid synthesis in the yeast Saccharomyces cerevisiae. Annu Rev Biochem 80, 859–883.

Cox JS, Chapman RE, Walter P (1997). The unfolded protein response coordinates the production of endoplasmic reticulum protein and endoplasmic reticulum membrane. Mol Biol Cell 8, 1805–1814.

Fei W, Shui G, Gaeta B, Du X, Kuerschner L, Li P, Brown AJ, Wenk MR, Parton RG, Yang H (2008). Fld1p, a functional homologue of human seipin, regulates the size of lipid droplets in yeast. J Cell Biol 180, 473–482.

Fei W, Shui G, Zhang Y, Krahmer N, Ferguson C, Kapterian TS, Lin RC, Dawes IW, Brown AJ, Li P, *et al.* (2011). A role for phosphatidic acid in the formation of "supersized" lipid droplets. PLoS Genet 7, e1002201.

Fleming JA, Lightcap ES, Sadis S, Thoroddsen V, Bulawa CE, Blackman RK (2002). Complementary whole-genome technologies reveal the cellular response to proteasome inhibition by PS-341. Proc Natl Acad Sci USA 99, 1461–1466.

Gietz RD, Sugino A (1988). New yeast-Escherichia coli shuttle vectors constructed with in vitro mutagenized yeast genes lacking six-base pair restriction sites. Gene 74, 527–534.
Gregor MF, Yang L, Fabbrini E, Mohammed BS, Eagon JC, Hotamisligil GS, Klein S (2009). Endoplasmic reticulum stress is reduced in tissues of obese subjects after weight loss. Diabetes 58, 693–700.
Guerra-Moreno A, Hanna J (2016). Tmc1 is a dynamically regulated effector of the Rpn4 proteotoxic stress response. J Biol Chem 291, 14788–14795.
Guerra-Moreno A, Isasa M, Bhanu MK, Waterman DP, Eapen VV, Gygi SP, Hanna J (2015). Proteomic analysis identifies ribosome reduction as an effective proteotoxic stress response. J Biol Chem 290, 29695–29706.
Hanna J, Hathaway NA, Tone Y, Crosas B, Elsasser S, Kirkpatrick DS, Leggett DS, Gygi SP, King RW, Finley D (2006). Deubiquitinating enzyme Ubp6 functions noncatalytically to delay proteasomal degradation. Cell 127, 99–111.
Hanna J, Waterman D, Isasa M, Elsasser S, Shi Y, Gygi S, Finley D (2014). Cuz1/Ynl155w, a zinc-dependent ubiquitin-binding protein, protects cells from metalloid-induced proteotoxicity. J Biol Chem 289, 1876–1885.
Hipp MS, Park SH, Hartl FU (2014). Proteostasis impairment in protein-misfolding and -aggregation diseases. Trends Cell Biol 24, 506–514.
Hummasti S, Hotamisligil GS (2010). Endoplasmic reticulum stress and inflammation in obesity and diabetes. Circ Res 107, 579–591.
Huyer G, Piluek WF, Fansler Z, Kreft SG, Hochstrasser M, Brodsky JL, Michaelis S (2004). Distinct machinery is required in Saccharomyces cerevisiae for the endoplasmic reticulum-associated degradation of a multispanning membrane protein and a soluble luminal protein. J Biol Chem 279, 38369–38378.
Jelinsky SA, Estep P, Church GM, Samson LD (2000). Regulatory networks revealed by transcriptional profiling of damaged Saccharomyces cerevisiae cells: Rpn4 links base excision repair with proteasomes. Mol Cell Biol 20, 8157–8167.
Kaufman RJ (1999). Stress signaling from the lumen of the endoplasmic reticulum: coordination of gene transcriptional and translational controls. Genes Dev 13, 1211–1233.
Kruegel U, Robison B, Dange T, Kahlert G, Delaney JR, Kotireddy S, Tsuchiya M, Tsuchiyama S, Murakami CJ, Schleit J, *et al*. (2011). Elevated proteasome capacity extends replicative lifespan in Saccharomyces cerevisiae. PLoS Genet 7, e1002253.
Leggett DS, Hanna J, Borodovsky A, Crosas B, Schmidt M, Baker RT, Walz T, Ploegh H, Finley D (2002). Multiple associated proteins regulate proteasome structure and function. Mol Cell 10, 495–507.
Mannhaupt G, Schnall R, Karpov V, Vetter I, Feldmann H (1999). Rpn4p acts as a transcription factor by binding to PACE, a nonamer box found upstream of 26S proteasomal and other genes in yeast. FEBS Lett 450, 27–34.
Metzger MB, Michaelis S (2009). Analysis of quality control substrates in distinct cellular compartments reveals a unique role for Rpn4p in tolerating misfolded membrane proteins. Mol Biol Cell 20, 1006–1019.
Ozcan U, Cao Q, Yilmaz E, Lee AH, Iwakoshi NN, Ozdelen E, Tuncman G, Görgün C, Glimcher LH, Hotamisligil GS (2004). Endoplasmic reticulum stress links obesity, insulin action, and type 2 diabetes. Science 306, 457–461.
Radhakrishnan SK, Lee CS, Young P, Beskow A, Chan JY, Deshaies RJ (2010). Transcription factor Nrf1 mediates the proteasome recovery pathway after proteasome inhibition in mammalian cells. Mol Cell 38, 17–28.
Radulovic M, Knittelfelder O, Cristobal-Sarramian A, Kolb D, Wolinski H, Kohlwein SD (2013). The emergence of lipid droplets in yeast: current status and experimental approaches. Curr Genet 59, 231–242.
Sá-Moura B, Funakoshi M, Tomko RJ Jr, Dohmen RJ, Wu Z, Peng J, Hochstrasser M (2013). A conserved protein with AN1 zinc finger and ubiquitin-like domains modulates Cdc48 (p97) function in the ubiquitin-proteasome pathway. J Biol Chem 288, 33682–33696.
Schuck S, Prinz WA, Thorn KS, Voss C, Walter P (2009). Membrane expansion alleviates endoplasmic reticulum stress independently of the unfolded protein response. J Cell Biol 187, 525–536.
Selvaraju K, Rajakumar S, Nachiappan V (2014). Identification of a phospholipase B encoded by the LPL1 gene in Saccharomyces cerevisiae. Biochim Biophys Acta 1842, 1383–1392.
Seufert W, Jentsch S (1990). Ubiquitin-conjugating enzymes UBC4 and UBC5 mediate selective degradation of short-lived and abnormal proteins. EMBO J 9, 543–550.
Shi Y, Chen X, Elsasser S, Stocks BB, Tian G, Lee BH, Shi Y, Zhang N, de Poot SA, Tuebing F, *et al*. (2016). Rpn1 provides adjacent receptor sites for substrate binding and deubiquitination by the proteasome. Science 351, 6275.
Shirozu R, Yashiroda H, Murata S (2015). Identification of minimum Rpn4-responsive elements in genes related to proteasome functions. FEBS Lett 589, 933–940.
Steffen J, Seeger M, Koch A, Krüger E (2010). Proteasomal degradation is transcriptionally controlled by TCF11 via an ERAD-dependent feedback loop. Mol Cell 40, 147–158.
Thibault G, Shui G, Kim W, McAlister GC, Ismail N, Gygi SP, Wenk MR, Ng DT (2012). The membrane stress response buffers lethal effects of lipid disequilibrium by reprogramming the protein homeostasis network. Mol Cell 48, 16–27.
Travers KJ, Patil CK, Wodicka L, Lockhart DJ, Weissman JS, Walter P (2000). Functional and genomic analyses reveal an essential coordination between the unfolded protein response and ER-associated degradation. Cell 101, 249–258.
Volmer R, Ron D (2015). Lipid-dependent regulation of the unfolded protein response. Curr Opin Cell Biol 33, 67–73.
Walter P, Ron D (2011). The unfolded protein response: from stress pathway to homeostatic regulation. Science 334, 1081–1086.
Wang CW (2015). Lipid droplet dynamics in budding yeast. Cell Mol Life Sci 72, 2677–2695.
Wu H, Ng BS, Thibault G (2014). Endoplasmic reticulum stress response in yeast and humans. Biosci Rep 34, e00118.
Xie Y, Varshavsky A (2001). RPN4 is a ligand, substrate, and transcriptional regulator of the 26S proteasome: a negative feedback circuit. Proc Natl Acad Sci USA 98, 3056–3061.